

100 Gbps over four pair balanced cabling

Albrecht M. Oehler, Katharina Seitz, Dieter Schicketanz

Reutlingen University

Reutlingen, Germany

+49-7121-271-5011 · Albrecht.Oehler@reutlingen-university.de

Alexander Franck, Yvan Engels

LEONI

Nürnberg, Germany

+49-4491-291-5048 · Alexander.Franck@lsc.leoni.com

Rainer Schmidt, Markus Witte

HARTING Electronics

Espelkamp, Germany

+49-30-565 82 782 · Rainer.Schmidt@HARTING.com

Abstract

Today 40 Gbps is in development at IEEE 802.3bq over four pair balanced cabling. In this paper, we describe a transmission experiment of 25 Gbps enabling either a single pair transmission of 25 Gbps over a 30 meter balanced cabling channel, or a 100 Gbps transmission via a four-pair balanced channel. A scalable matrix modeling tool is introduced which allows the prediction of transmission characteristics of a channel taking mode conversion into account. We applied this tool to characterize PCB-channels including the magnetics and PCB for a four-pair 100 Gbps transmission. We evaluated prototype cables and connecting hardware for frequencies up to 2 GHz and beyond. Finally we investigated possible line encoding schemes and provide measurement results of a transmission over 30 m with a data rate of 25 Gbps per twisted pair.

Keywords: Balanced cabling; 100 Gbps; matrix modeling; prototype cables; prototype fixtures; line encoding.

1. Introduction

The demand for higher data rates over 100 Ohm balanced cabling in data centers drives IEEE 802.3 to increase its Ethernet data rate to 40 Gbps (40GBASE-T). To investigate the future proof and the efficiency of balanced cabling we present experiments of transmissions at data rates up to 25 Gbps resulting in 100 Gbps for four-pair cabling.

In the first part of this paper we present a matrix modeling tool which allows the investigation of the transmission characteristics of balanced cabling channels, consisting of balanced cables and connecting hardware. We take into account both, differential and common mode. The model presented herein is scalable and thus allows for handling any number N of pairs (see fig.1). [1]

The second part of this paper addresses line encoding. Pulse Amplitude Modulation (PAM-32) and Carrierless Amplitude and Phase (CAP-1024) line encoding are discussed for a 25 Gbps data rate per pair. The choice of the line encoding is based on minimizing the symbol rate and therefore minimizing the

transmission bandwidth when simultaneously taking the noise floor into account.

The third part covers the transmission channel. First the channel's spectral characteristics of a PCB-channel including the decoupling magnetics and the PCB traces of the terminal equipment is predicted by means of the above mentioned modeling tool. This allows one to predict the performance of a so-called PCB-channel. Secondly experimented flexible and solid prototype cables, with individually shielded pairs, as well as various types of test fixtures and connectors are introduced. Finally channel measurements provide results..

The last part shows the measurement results of 25 Gbps per pair transmission experiments allowing a 100 Gbps transmission over a four pair channel with a 30 meter length. In addition an equalizer was developed, for the purpose of flattening the transmission characteristic of a twisted pair. Thus a usable bandwidth of more than 2 GHz was achieved.

2. Matrix Modeling

2.1 Mixed-mode S-matrix for a cable or a connector

A cable with N twisted pairs is shown in Fig.1. Pairs' terminals (two wires per terminal) are ascribed index n ($1 \leq n \leq 2N$). Mixed-mode S-matrix $[S]$ for this cable is a relationship between the modal waves marked in Fig.2-1; these waves are defined hereafter.

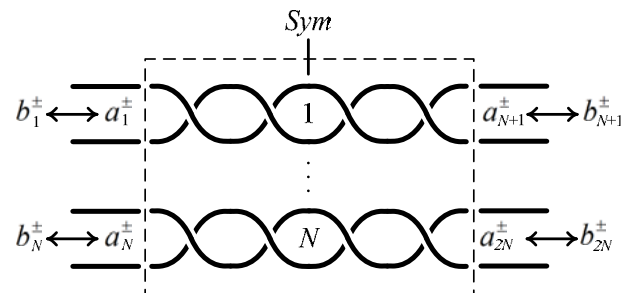


Figure 2-1: Cable with N twisted pairs

Pair terminal n is shown in Fig.2. Let v_n and v'_n be the respective potential drops in plane Pl , between the wires of this terminal and a third conductor $C3$. The latter is the pair's *individual* shield, if there is one. If there is none, $C3$ is the *overall* cable's shield. Let i_n and i'_n be the respective currents which flow on these wires, inwards through Pl .

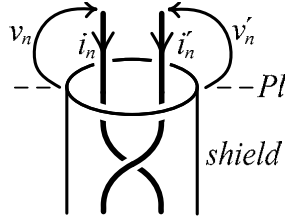


Figure 2-2: Voltages and currents at terminal No. n

Define balanced voltage and current

$$v_n^- = v_n - v'_n, \quad i_n^- = i_n / 2 - i'_n / 2 \quad (1)$$

and define unbalanced voltage and current

$$v_n^+ = v_n / 2 + v'_n / 2, \quad i_n^+ = i_n / 2 + i'_n / 2. \quad (2)$$

Define balanced waves (– superscript) and unbalanced waves (+ superscript), respectively incident on terminal n (a_n^\pm) and outgoing from this terminal (b_n^\pm) :

$$\begin{cases} a_n^\pm = v_n^\pm / 2\sqrt{Z^\pm} + \sqrt{Z^\pm} i_n^\pm / 2 \\ b_n^\pm = v_n^\pm / 2\sqrt{Z^\pm} - \sqrt{Z^\pm} i_n^\pm / 2 \end{cases} \quad (3)$$

where Z^\pm are the reference impedances of the balanced and unbalanced modes, respectively, for *all* the cables and connectors.

$Z^- = 100\Omega$ is common; Z^+ will be commented upon, later.

Define $4N$ -size modal vectors

$$\begin{cases} \mathbf{a} = [a_1^- \dots a_{2N}^- \ a_1^+ \dots a_{2N}^+]^T \\ \mathbf{b} = [b_1^- \dots b_{2N}^- \ b_1^+ \dots b_{2N}^+]^T \end{cases} \quad (4)$$

These vectors have been transposed (superscript T), for the sake of editing. $4N \times 4N$ matrix $[\mathbf{S}]$ serves to express \mathbf{b} in terms of \mathbf{a} :

$$\mathbf{b} = [\mathbf{S}] \mathbf{a} \quad (5)$$

The above applies to connectors, also.

The commercial four-port network analysers measure not more than *two* pair terminals at a time. They usually index the S_{ij} elements of $[\mathbf{S}]$ in the following way:

$$\begin{bmatrix} b_1^- \\ b_2^- \\ b_1^+ \\ b_2^+ \end{bmatrix} = \underbrace{\begin{bmatrix} S_{11}^{--} & S_{12}^{--} \\ S_{12}^{--} & S_{11}^{--} \\ S_{11}^{+-} & S_{12}^{+-} \\ S_{12}^{+-} & S_{11}^{+-} \\ S_{11}^{++} & S_{12}^{++} \\ S_{12}^{++} & S_{11}^{++} \end{bmatrix}}_{[\mathbf{S}]} \begin{bmatrix} a_1^- \\ a_2^- \\ a_1^+ \\ a_2^+ \end{bmatrix}, \quad (6)$$

where reciprocity ($S_{ij} = S_{ji}$, $i, j = 1 \dots 4N$) and cable's

symmetry about plane *Sym* in Fig.1 ($S_{ii} = S_{i+N, i+N}$,

$i = 1 \dots N$) have been accounted for. The S_{ij}^{+-} terms quantify

conversion between balanced and unbalanced modes. There is no

such conversion if balance is perfect ($S_{ij}^{+-} = 0$, $i, j = 1, 2$). In

this case, the upper left-hand side quarter of $[\mathbf{S}]$ characterises balanced operation *fully*, in a relationship that is well known to the engineer:

$$\begin{bmatrix} b_1^- \\ b_2^- \end{bmatrix} = \begin{bmatrix} S_{11}^{--} & S_{12}^{--} \\ S_{12}^{--} & S_{11}^{--} \end{bmatrix} \begin{bmatrix} a_1^- \\ a_2^- \end{bmatrix}. \quad (7)$$

When $N \geq 2$, ports 1&2 of the network analyser at hand are connected to, say terminal n . Analyser's ports 3&4 are connected to terminal n' , amongst the other $2N - 1$ terminals (Fig.1). An

4×4 S-matrix (6) is measured; ports 3&4 are then switched to an other terminal, and so forth... The cable's $4N \times 4N$ S-matrix is a concatenation of the 4×4 matrices thus measured. The same procedure is followed when a connector is measured, with the difference that, in general, (6) S_{ii} differs from $S_{i+N, i+N}$, then.

While pair terminals n and n' are connected to the network analyser, the other terminals must be loaded in such a way, that incident waves (3) a_n^\pm ($n'' \neq n, n'$) be cancelled.

2.2 Mixed-mode chain matrix

Ultimately, one wishes to predict the behaviour of cables and connectors, cascaded as shown in Fig.2-3, by means of a mixed-mode S-matrix $[\mathbf{S}_{cas}]$ like the one in (5).

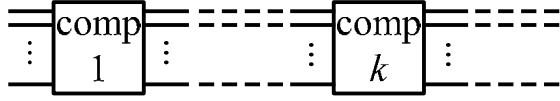


Figure 2-3: Cascade of components e.g. cables and connectors

The S-matrices of the links in this figure lend themselves to no easy computation of $[S_{cas}]$, such as a multiplication of matrices.

For the purpose of inducing such a simple operation eventually, so-called chain matrix $[T]$ is derived hereafter, from S-matrix $[S]$ of a general component from Fig.2-3.

$$\mathbf{c} = [T] \mathbf{d}, \quad (8)$$

where $4N$ -size vector \mathbf{c} group together the waves that are incident on, or come out of the *left-hand* side of this component:

$$\mathbf{c} = [b_1^- a_1^- \dots b_N^- a_N^- b_1^+ a_1^+ \dots b_N^+ a_N^+]^T \quad (9)$$

(refer to Fig.1 for indexing) and where $4N$ -size vector \mathbf{d} group together the waves that are incident on, or come out of the *right-hand* side:

$$\mathbf{d} = [a_{N+1}^- b_{N+1}^- \dots a_{2N}^- b_{2N}^- a_{N+1}^+ b_{N+1}^+ \dots a_{2N}^+ b_{2N}^+]^T \quad (10)$$

$[T]$ is obtained as

$$\mathbf{c} = \underbrace{\left(\begin{aligned} &([X_{ca}] + [X_{cb}][S]) \cdot \\ &([X_{da}] + [X_{db}][S])^{-1} \end{aligned} \right)}_{[T]} \mathbf{d}. \quad (11)$$

where

$$[X_{ca}] = \begin{bmatrix} [P] & [0] & [0] & [0] \\ [0] & [0] & [P] & [0] \end{bmatrix}, \quad (12)$$

$$[X_{cb}] = \begin{bmatrix} [Q] & [0] & [0] & [0] \\ [0] & [0] & [Q] & [0] \end{bmatrix}, \quad (13)$$

$$[X_{da}] = \begin{bmatrix} [0] & [Q] & [0] & [0] \\ [0] & [0] & [0] & [Q] \end{bmatrix}, \quad (14)$$

$$[X_{db}] = \begin{bmatrix} [0] & [P] & [0] & [0] \\ [0] & [0] & [0] & [P] \end{bmatrix}. \quad (15)$$

are $4N \times 4N$ matrices, and where

$$[P] = \begin{bmatrix} 0 & 0 & 0 & \dots & 0 \\ 1 & 0 & 0 & \dots & 0 \\ 0 & 0 & 0 & \dots & 0 \\ 0 & 1 & 0 & & 0 \\ \vdots & & \ddots & & \vdots \\ 0 & \dots & 0 & 1 & 0 \\ 0 & \dots & 0 & 0 & 0 \\ 0 & \dots & 0 & 0 & 1 \end{bmatrix} \quad (16)$$

and

$$[Q] = \begin{bmatrix} 1 & 0 & 0 & \dots & 0 \\ 0 & 0 & 0 & \dots & 0 \\ 0 & 1 & 0 & \dots & 0 \\ 0 & 0 & 0 & & 0 \\ \vdots & & \ddots & & \vdots \\ 0 & \dots & 0 & 0 & 0 \\ 0 & \dots & 0 & 0 & 1 \\ 0 & \dots & 0 & 0 & 0 \end{bmatrix} \quad (17)$$

are $2N \times N$ matrices. $[0]$ is the $2N \times N$ zero-matrix.

2.3 Cascade's S-matrix

Going from left to right in Fig.2-3, the (10) \mathbf{d} vector of a component is the (9) \mathbf{c} vector of the next one, so one may multiply the components' chain matrices, in order to obtain cascade's chain matrix

$$[T_{cas}] = [T_1][T_2] \dots \quad (18)$$

Since (18) expresses $[T_{cas}]$ in terms of $[S_{cas}]$, as much as $[T]$ in terms of $[S]$, one may revert this equation, in order to obtain

$$[S_{cas}] = \frac{([T_{cas}][X_{db}] - [X_{cb}])^{-1}}{([X_{ca}] - [T_{cas}][X_{da}])} \quad (19)$$

Not only does (19) say how much energy converts between balanced and unbalanced modes, through a cascade whose balance is not perfect all the way; it also predicts what happens when the signal generated by the *transmitter* that is plugged at one end of the cascade, or the signal reflected by the *receiver* at the other end, is not well balanced.

2.4 Consistent reference impedances

Suppose that modal S-matrix $[S']$ of one of the components in Fig.2-3, was measured at a manufacturer's where $Z^{\pm'} \neq Z^{\pm}$ were the reference impedances. Since the matrices involved in (18) must refer to same Z^{\pm} , $[S']$ is converted into $[S]$ which refers to Z^{\pm} , before (11,18,19) are applied. $[S]$ is derived from $[S']$ as follows. Define modal vectors (4) \mathbf{a}', \mathbf{b}' whose components (3) $a_n^{\pm'}, b_n^{\pm'}$ refer to $Z^{\pm'}$:

$$\begin{cases} a_n^{\pm'} = v_n^{\pm} / 2\sqrt{Z^{\pm'}} + \sqrt{Z^{\pm'}} i_n^{\pm} / 2 \\ b_n^{\pm'} = v_n^{\pm} / 2\sqrt{Z^{\pm'}} - \sqrt{Z^{\pm'}} i_n^{\pm} / 2 \end{cases} \quad (20)$$

Express v_n^{\pm}, i_n^{\pm} in terms of $a_n^{\pm'}, b_n^{\pm'}$ and use in (3) to express a_n^{\pm}, b_n^{\pm} in terms of $a_n^{\pm'}, b_n^{\pm'}$,

$$\begin{cases} 2\mathbf{a} = [\Sigma] \mathbf{a}' + [\Delta] \mathbf{b}' \\ 2\mathbf{b} = [\Delta] \mathbf{a}' + [\Sigma] \mathbf{b}' \end{cases} \quad (21)$$

where $\mathbf{b}' = [S'] \mathbf{a}'$, as in (5). $[\Sigma]$ and $[\Delta]$ are diagonal matrices whose n^{th} diagonal terms are, respectively, $\Sigma_{nn} = x_n + 1/x_n$ and $\Delta_{nn} = x_n - 1/x_n$, with $x_{n \leq 2N} = \sqrt{Z^{-'}/Z^{-}}$ and $x_{n > 2N} = \sqrt{Z^{+'}/Z^{+}}$. Replace \mathbf{b}' in (21) with $[S'] \cdot \mathbf{a}'$:

$$\mathbf{b} = \underbrace{([\Delta] + [\Sigma][S'])([\Delta] + [\Sigma][S'])^{-1}}_{[S]} \mathbf{a} \quad (22)$$

3. Line Encoding

This part deals with possible approaches for line encoding. Line encoding consists of representing the digital logic by using the physical attributes of the channel. It is used to transfer information. For the balanced transmission of 100 Gbps we developed two different approaches. Both are based on a carrierless multilevel code. The aim is to minimize the symbol rate and in addition to that to minimize the transmission bandwidth.

The first approach is a Pulse Amplitude Modulation (PAM 32) and the second one is Carrierless Amplitude and Phase Modulation (CAP 1024). For both line encodings we used a

special formed impulse. The used Raised-Cosine impulse is defined as

$$g_i(t) = \frac{\sin\left[\frac{\pi t}{T_s}(1-\alpha)\right] + \frac{4\alpha t}{T_s} \cos\left[\frac{\pi t}{T_s}(1-\alpha)\right]}{\frac{\pi t}{T_s} \left[1 - \left(\frac{4\alpha t}{T_s}\right)^2\right]} \quad (23)$$

with $\alpha = 0.15$.

The parameter T_s defines the symbol period [2].

3.1 PAM-32

For the Pulse Amplitude Modulation we have chosen 32 relative levels of the amplitude. Each amplitude represents a symbol with 5 bits. Therefore the symbol period is five times longer than the bit period. For the transmission of 25 Gbps over one twisted pair of a four pair channel the symbol rate is 5 GBd. The usual sinusoidal carrier oscillation is replaced by the Raised-Cosine impulse.

3.2 CAP 1024

The second approach is the Carrierless Amplitude and Phase Modulation. Each component, the in-phase impulse and the quadrature impulse, has 32 different levels of amplitude. Each combination of the amplitude of the in-phase and the quadrature impulse represents a symbol with 10 bits. For the transmission of 25 Gbps over one twisted pair of a four pair channel the symbol rate is 2.5 GBd.

The in-phase impulse is defined as

$$g_c(t) = g_i(t) \cdot \cos(2\pi \cdot f_c \cdot t) \quad (24)$$

and the quadrature impulse is defined as

$$g_s(t) = g_i(t) \cdot \sin(2\pi \cdot f_c \cdot t). \quad (25)$$

Both impulses with the Raised-Cosine impulse $g_i(t)$ and a center frequency of $f_c = 2.5$ GHz [2]. The result is a transmitted signal with

$$s(t) = g_c(t) + g_s(t). \quad (26)$$

4. Transmission Channel

4.1 Channel Definitions

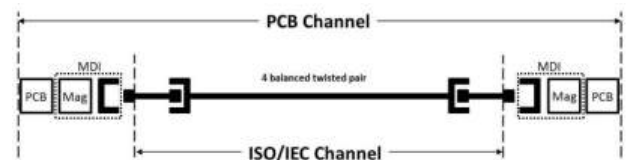


Figure 4-1: ISO/IEC Channel and PCB Channel

The ISO/IEC cabling channel used for these experiments resembled the Channel definition presented in [3].

The PCB-Channel includes the media dependent interface (MDI), consisting of the connector (device connectivity) and the magnetics performing DC-separation and common mode rejection., the PCB-traces which is the carrier of the MDI and the cable link with the connectors.

The Channel setup consists of 26 m horizontal cable, 2 x2 m cord and the needed connections in between.

The cables and connections used are described in the following clauses. The maximum frequency of the channels presented in [3] is 1600 MHz with an option to increase it to 2000 MHz.

For the transmission experiment up to 3 GHz only 1 pair of a 30m cable was used connected to a prototype equalizing amplifier.

The PCB channel adds to the ISO/IEC cabling channel the PCB and the connections at each end, it excluded any electronics. Examples of transmission performance of the PCB Channel up to 2000 MHz can be found at the IEEE 802.3bq public homepage in [4] and [5].

4.2 Cables

Today common shielded twisted pair data cables provide and ensure a minimum transmission bandwidth of 1GHz. This cable meets the cable category 7_A performance . Due to the encoding of the signals the full frequency range is important so that the cable need to guarantee a stable and smooth insertion loss, high return loss and small near-end and far-end crosstalk. The near-end and far-end crosstalk between the individually screened twisted pair cables is usually not causing any problems.

One has to take care if the pair leaves the perfect boundaries in a shielded twisted pair cable for the connection to a test fixture or connector.

For this project the goal was to provide a physical medium with the best characteristics as possible, e.g. with respect to insertion loss and return loss. The cable design parameters need to be fitted for a smooth and low attenuation and a good impedance matching. At least the whole production process must be optimized accurately.

In the first step a cable with a total bandwidth of 1.5 GHz has been tested and evaluated. Above the frequency limit of 1.5GHz the cable can't be used due to the design and process engineering features. Based on this cable other variants have been developed. First mathematical recommendations regarding the bandwidth resulted in a reach of the 2 GHz. The first cable prototypes showed a non stable attenuation trend of a 50m cable which violated the extrapolated limit line.

In fig.4-2 plot the insertion loss with above mentioned unsettled trend is shown and in fig.4-3 the return loss is shown with frequency suck outs (600-800MHz) long before the desired 2 GHz.

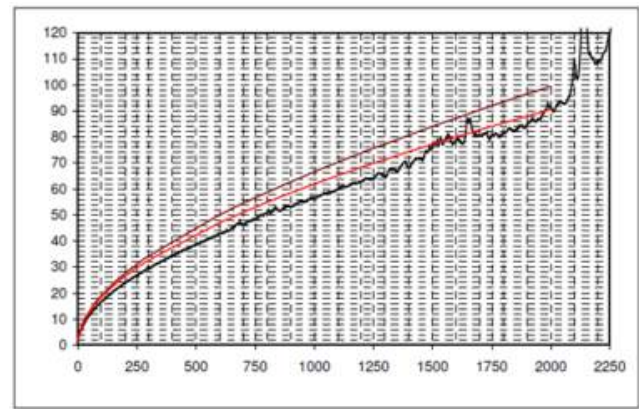


Figure 4-2: Insertion loss results

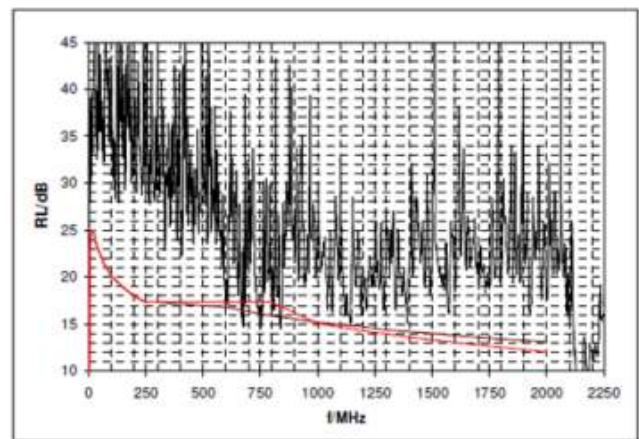


Figure 4-3: Return loss results

After different re-designs of the cable, without significant cable diameter enlargement, it was possible to reduce the weakening of individual pairs and the total cable.

In the following plots one of the latest 2 GHz prototypes (50m) is shown.

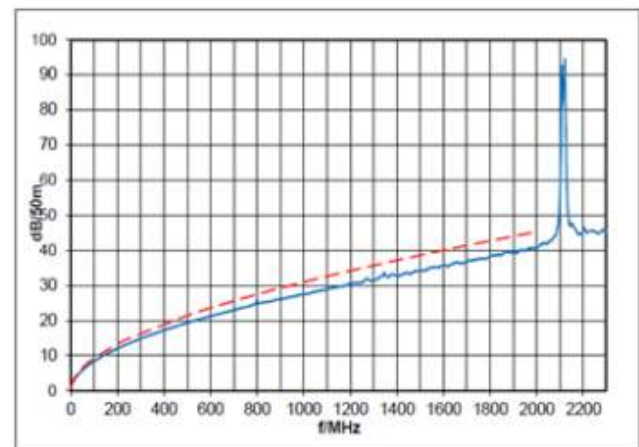


Figure 4-4: Insertion loss 2 GHz cable

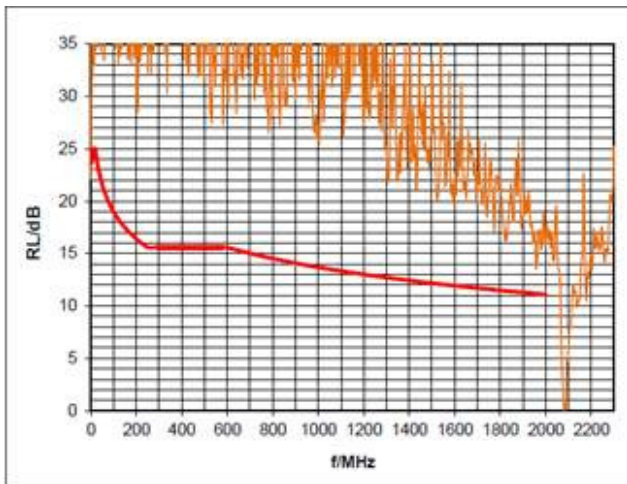


Figure 4-5: Return loss 2GHz cable

A smooth insertion loss with a value of 41 dB at 2 GHz and return loss with a value of 17 dB at 2 GHz provide an initial basis for further tests in the project.

After further project investigation the boundary conditions have been changed. For further assumptions a shielded twisted pair cable will provide with a bandwidth of 2.5 GHz and beyond and a cable length of 30 m

4.3 Connecting Hardware

The challenge for connecting hardware components in a 2.5 GHz channel is to provide sufficient transmission characteristics over this bandwidth.

To qualify a suitable connector type, mated pair configurations had to be considered in detail that means plug and jack (male and female connectors) at first.

Based on the long term experience of the experts involved with this analysis, a selection of existing connector types was made. With the expectation to fulfil the tough requirements in a 2.5 GHz channel.

In a first step the following connector types (existing interfaces) had been chosen for further study:

- Copper connector acc. IEC 61076-3-104 (Tera connector specified up to 1000MHz, cat.7_A)
- Copper connector acc. IEC 61076-3-110 (ARJ connector specified up to 1000MHz, cat.7_A)
Note: GG45 without switch contacts has a very similar performance to ARJ
- Copper connector acc. IEC 60603-7-51 (RJ45 screened connector specified up to 500MHz, cat.6_A)
- Copper connector acc. IEC 61076-2-109 (M12 X-coded connector specified up to 500MHz, cat.6_A)

In the course of the discussion an additional interface was selected for inspection – SFP (acc. SFF-8432 and similar), which could be used in device connectivity.

The mentioned connectors had been measured under laboratory conditions by terminating the mated interfaces on a cable clamp termination unit for all four pairs and measuring the most important transmission parameters like return loss (RL), insertion loss (IL), near-end and far-end crosstalk (NEXT and FEXT) a.o.m. up to the frequency range of 2.5 GHz.

For testing a RF switch matrix had been used in conjunction with a VNA (vectorial network analyzer) and PLTS (Physical Layer

Test System) software. To minimize measurement errors and to get reliable and reproducible test results the test arrangement and method was double-checked by a round-robin test between all project partners.



Figure 4-6: Cable clamp termination unit with test object

The test results for the considered transmission parameters for the four connector types specified in IEC delivered a ranking in performance convenient for the 2.5 GHz channel configuration.

Connector designs specified today acc. cat.7_A provide best capabilities for future high speed transmission with a bandwidth of 2.5 GHz or more followed by the circular connectors in M12 design.

The today RJ45 connector design is very limited in delivering acceptable transmission performance for a 2.5 GHz channel.

Beside the amount of transmission parameters considered and the test results delivering clear messages regarding the possible performance capabilities the return loss, cross talk and balance of connector designs are the most critical parameters.

In the following figures some of the test results are shown in detail:

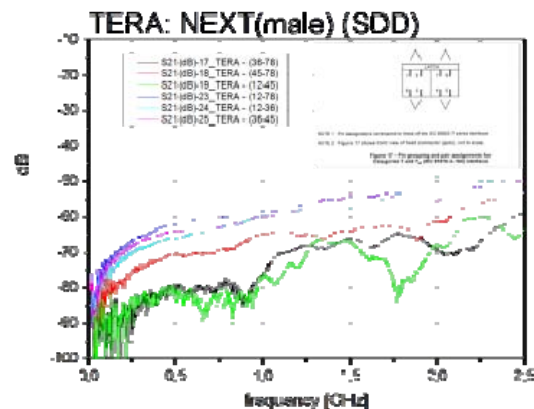


Figure 4-7: NEXT results for connector type acc. IEC 61076-3-104

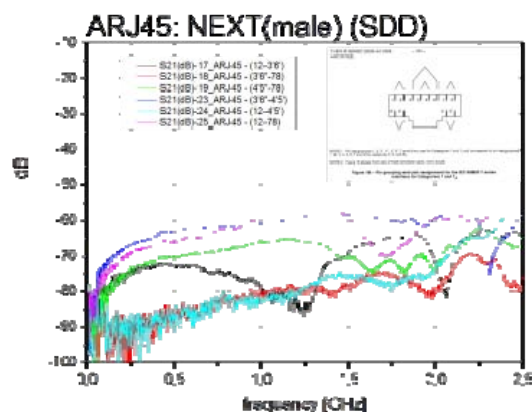


Figure 4-8: NEXT results for connector type acc. IEC 61076-3-110

4.4 Channel Measurements

A WireXpert 4500 from Psiber Data was used to measure Channels up to 2400 MHz. The limit lines shown are the Class II limits of [3]. It was set up as explained in 4.1 with selected components of 4.2 and 4.3. The results are similar for connection A or connection B.

Main Parameters of a selected channel:

- For insertion loss of the cable see Fig 5-1
- Return loss of channel: Fig. 4-9
- Powersum NEXT (PSNEXT) of channel, see Fig 4-10

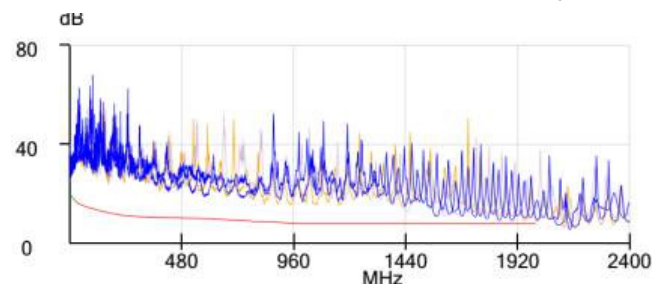


Figure 4-9: 30 m channel return loss

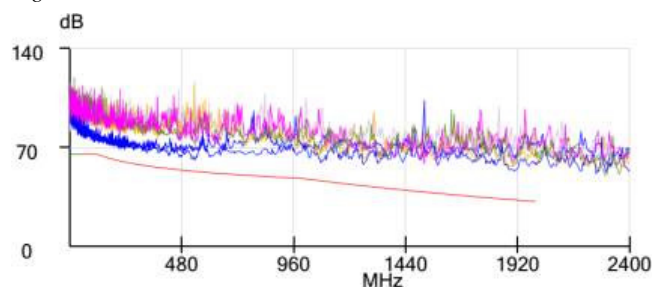


Figure 4-10: 30m channel powersum NEXT

5. Data Transmission

5.1 Channel

The setup used for the transmission experiment consisted of 30 m of cable and a prototype equalizing amplifier.

For the spectral measurement a vector network analyzer 5081B from Agilent was used.

Fig 5-1 shows the measurements of the insertion loss.

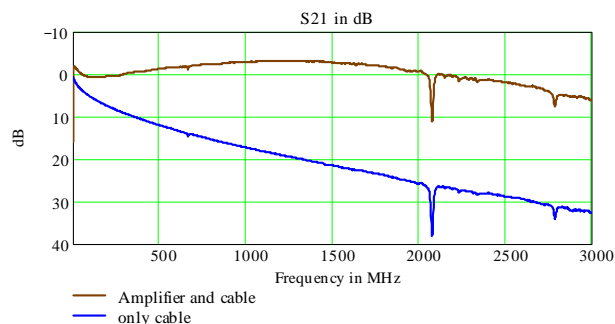


Figure 5-1: Insertion loss of the pair used in the transmission experiment. Blue (lower line): 30 m cable only, Brown (upper line): cable and equalizing amplifier

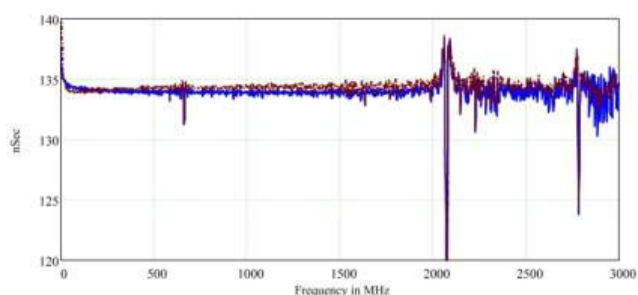


Figure 5-2: Group Delay: Blue (solid line): 30 m cable only, Brown (dotted line): cable and equalizing amplifier

5.2 Test results PAM32 – 25Gbps

To test the transmission of 25 Gbps we used two different measurement setups. The Tektronix Arbitrary Waveform Generator AWG 70001A generated the signal. For the first measurement setup the AWG is directly connected with the Tektronix Sampling Oscilloscope CSA 8000. For the second measurement setup the symmetric outputs of the AWG are connected with one pair of the cable. At the end of the cable the equalizing amplifier are connected. The symmetric outputs of the amplifier are connected to the Tektronix Sampling Oscilloscope CSA 8000.

For the first measurement we used a sequence of signals including all 32 different levels of amplitude. The following figures shows the transmitted $s(t)$ and received $r(t)$ test sequence.

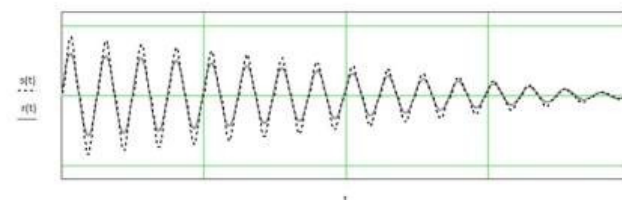


Figure 5-3: Transmitted (dotted line) and received (solid line) PAM 32 signal (1.6 ns per horizontal division, 500 mV per vertical division)

This sequence could be decoded.

Further line encodings, arbitrary bit sequences and bit error rate measurements are in progress.

6. Conclusion

In this paper a modeling tool is introduced allowing the prediction of PCB-channels. Balanced cabling channels have been assembled using prototype cables and connecting hardware allowing a transmission bandwidth with an upmost frequency of 2.5 GHz and beyond. Test sequences with 25 Gbps per pair have been transmitted allowing 100 Gbps over a 30 meter four-pair channel.

7. Acknowledgments

This work was supported by the German Federal Ministry for Economic Affairs and Energy on the basis of a decision by the German Bundestag.

Gefördert durch:



aufgrund eines Beschlusses
des Deutschen Bundestages

The authors would like to thank Dr. Denis Jaisson for his contribution to part 2.

8. References

- [1] D. Jaisson, A. Oehler, A. Franck, M. Schulte, D. Schicketanz, "Impact of the common mode for high data rate transmission over balanced cabling", ITG-Fachbericht 245, 62 - 69, Berlin: VDE-Verlag, 2013.
- [2] The ATM Forum - Technical Committee, "155.52 Mb/s Physical Layer Specification for Category-3 Unshielded Twisted Pair" - af-phy-0047.00: November, 1995.
- [3] ISO/IEC technical report 11801-99-1: Guidance for balanced cabling in support of at least 40 Gbit/s data transmission.
- [4] http://www.ieee802.org/3/bq/public/jan14/franck_3bq_01a_0114.pdf
- [5] http://www.ieee802.org/3/bq/public/channelmodeling/Channeladhoc_March4_Schicketanz.pdf

9. Authors



Prof. Dr. Albrecht Oehler
e-mail see title

Albrecht Oehler is a professor in Information and Communication Technologies at the Reutlingen University since 1995. His research interests are modeling, high frequency measurements and data transmission within Local Area Networks. He

received his Diplom-Ingenieur at the University of Kaiserslautern. Afterwards he was engaged at the Siemens AG central research and communication networks. His Ph.D. Albrecht Oehler received at the University of Kaiserslautern in fiber optics. He is convenor of the international working group in charge of customer premises cabling ISO/IEC JTC 1 SC 25/WG 3.



M.Sc. Katharina Seitz
e-mail: Katharina.seitz@t-online.de

Katharina Seitz studied Business Engineering and graduated with a Bachelor degree at the Baden-Wuerttemberg Cooperative State University Stuttgart. Followed by a Master of Science degree at the Reutlingen University. Her Masterthesis was about line encoding for 25 Gbps over symmetrical twisted pair.



Dr. Dieter Schicketanz
e-mail: dieter.schicketanz@t-online.de

Dr. Dieter Schicketanz began with fiber optics 1970 at R&D at Siemens in Munich. In 1984 he worked for 4 years at SIECOR in Hickory NC. Returning to Munich he worked first in analog TV transmission over single mode fibre to change topic in 1992 towards mainly copper usage in buildings. Since 2005 he consults different standardization bodies.



M. ENG.. Alexander Franck
e-mail see title

Alexander Franck received his Master of Science degree in 2011 in electrical engineering in the field of telecommuni-

cation (RF) at the University of Applied Sciences of Aachen/Germany. Followed by his Master thesis he started to work at LEONI Kerpen GmbH in the R&D: Here, he was involved in development for data cables before continuing to work at LEONI Special Cable GmbH in the field of high speed assemblies for active and passive QSFP+ (40G/100G) and SFP+.

His present work includes the development of the assemblies, PCB-Design, RF measurements and 3D EM simulations.



Dipl.-Ing. Yvan Engels
e-mail: yvan.engels@leoni.com

Yvan Engels born on 30.01.1954 in Eupen/Belgium

Head of Product Management Datacom until 31.07.2013 and Strategic Market Development and Standardisation since 01.08.2013 (BU Infrastructure&Datacom) at LEONI KERPEN GmbH

University studies of communication engineering at FH-Aachen/Germany
Member of international and national

standardisation bodies and associations:
ISO/IEC JTC1 SC25 WG3, GUK 715.3, GUK 715.3.7
EDC/TC, BitKom, BGNW, VIRZ
Author of numerous articles in datacom and telecommunication journals.



Dipl.-Ing. Rainer Schmidt
e-mail see title

Rainer Schmidt born on 1st of July 1958 in Berlin/Germany. Received his diploma in information technology at Technical University Dresden/Germany in

1982 and started his career as Service Engineer for distributed process computer systems.

Starting 1992 he filled leading positions in Product Management/Marketing for structured cabling systems in KRONE. 2006 he moved to HARTING and took over the head of Product Management for industrial cabling systems. Today he is Business Development Manager for industrial cabling within the GBU Electronics of the HARTING Technology Group.

Rainer Schmidt is member of international and national standardization bodies and associations like ISO/IEC JTC1 SC25 WG3, IEC SC65C JWG10, GUK 715.3 a.o.m.



Dipl.-Ing. (FH) Markus Witte
e-mail:

markus.witte@HARTING.com
Markus Witte received his Diplom-Ingenieur (FH) degree as an engineer in Electrical Communications Engineering at the University of Applied Sciences Osnabrück in 1998. He has over 15 years of professional and management experience within the HARTING Technology group.

Markus Witte has significant experience with field solver based modeling of RF- and high speed interconnects, digital system simulation and development of test fixtures and reference backplanes and PCB's for compliance tests.